JCTC Journal of Chemical Theory and Computation

Article

pubs.acs.org/JCTC

Quantum Entanglement and Chemical Reactivity

M. Molina-Espíritu,[*,†] R. O. Esquivel,[*,†,‡] S. López-Rosa,[*,⊥,‡] and J. S. Dehesa[*,§,‡]

[†]Departamento de Química, Universidad Autónoma Metropolitana, 09340, México, D.F., México

[‡]Instituto Carlos I de Física Teórica y Computacional and [§]Departamento de Física Atómica, Molecular y Nuclear, Universidad de Granada, 18071 Granada, Spain

[⊥]Departamento de Física Aplicada II, Universidad de Sevilla, 41012 Sevilla, Spain

Supporting Information

ABSTRACT: The water molecule and a hydrogenic abstraction reaction are used to explore in detail some quantum entanglement features of chemical interest. We illustrate that the energetic and quantum-information approaches are necessary for a full understanding of both the geometry of the quantum probability density of molecular systems and the evolution of a chemical reaction. The energy and entanglement hypersurfaces and contour maps of these two models show different phenomena. The energy ones reveal the well-known stable geometry of the models, whereas the entanglement ones grasp the chemical capability to transform from one state system to a new one. In the water molecule the chemical reactivity is witnessed through quantum entanglement as a local minimum indicating the bond cleavage in the dissociation process of the molecule. Finally, quantum entanglement is also useful as a chemical reactivity descriptor by detecting the transition state along the intrinsic reaction path in the hypersurface of the hydrogenic abstraction reaction corresponding to a maximally entangled state.

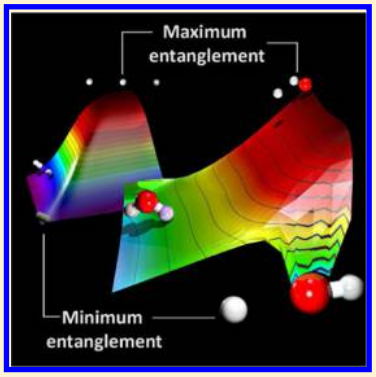

1. INTRODUCTION

The phenomenon of entanglement is one of the most fundamental aspects of the quantum mechanical description of nature.[1] Despite the fact that the first experiments regarding entanglement have been performed using photons and electronic spins, entanglement with the massive particles chemists deal with is also of great interest. In this context, information theory has become the natural framework in which entanglement and related phenomena can be defined and properly studied.[2] In the last years, an increasing interest has arisen in studying biological processes through the formalism of quantum information theory,[3−6] where the chemical phenomena obviously play a crucial role. It is therefore clear that the concepts and tools of quantum information are entering the sphere of chemical interest.[7−11] Consequently, it is imperative for both quantum information theorists and theoretical chemists to concern themselves with the entanglement features exhibited by chemical systems and processes.[12]

It must be realized that quantum entanglement is not just a fashionable research topic, it is a fundamental concept of quantum physics that plays a deep role within all applications of quantum mechanics involving composite systems (e.g., problems directly related with molecular systems and chemical processes as mentioned earlier). In previous work, the amount of entanglement of the ground state and of the first few excited states of helium was assessed by employing high-quality state-of-the-art wave functions.[13−15] Other interesting results concerning quantum entanglement in atomic and related systems have been reported in.[16−32] The quantum entanglement-related aspects of the dissociation process of homo- and heteronuclear diatomic molecules have been investigated in.[33] Recently, orbital entanglement has been employed to qualitative understanding of bond-forming and bond-breaking processes.[34,35] Further, the von Neumann entropy has been employed to locate the quantum critical point in low-dimensional spin or Fermionic models.[36] Other related tools have been recently employed in quantum chemistry to locate transitions in the potential energy curve of the ionic−covalent avoided crossing in LiF[37] and on pseudo-one-dimensional systems in order to investigate metal−insulator like transition.[38]

The motivation for the exploration of the entanglement properties of chemical systems is manifold. Generally speaking, if two particles are in an entangled state, then even if the particles are physically separated by a large distance, they behave in some respects as a single entity rather than as two separate entities. A natural mechanism generating entanglement takes place when a former unit dissociates into simpler subsystems. This kind of processes are known quite well in chemistry. So, apart from its basic relevance for the foundations of physics, entanglement has necessarily to play an important role in chemistry too. Although information entropies have been used for a variety of studies in chemistry,[39] applications of entanglement measures in chemical systems are very scarce. For instance, in recent studies the relation between transition state (TS) in an IRC (intrinsic reaction path) chemical reaction and

Received: April 24, 2015
Published: October 8, 2015

DOI: 10.1021/acs.jctc.5b00390
J. Chem. Theory Comput. 2015, 11, 5144−5151

quantum entanglement has been analyzed in order to define a new chemical state known as *Maximum Entangled Transition State* (METS), which has been linked to chemical reactivity[40]

Traditionally, the concept of reactivity has been associated with a large number of chemical properties, e.g. hardness, activity, electronegativity, chemical potential, etc., which measure the extent at which chemical systems can interact.[41] However, there is no simple concept which can describe uniquely this chemical phenomenon. Interestingly, quantum entanglement seems to be associated with the general notion of reactivity as a measure of chemical change, i.e., the capacity to transform a chemical species from a specific state to a new one. Worthy to mention is the fact that despite classical IT has been proven to be useful to interpret several aspects of chemical phenomena;[39,42] to the best of our knowledge, there are no studies related to quantum IT applied to chemical reactivity. Considering that quantum entanglement is one of the most striking features of nature that accounts for a new type of physical correlations between subsystems that have no classical analogs and that chemical systems must possess some degree of entanglement, it is of paramount importance to analyze the possible link between the quantum entanglement and the chemical stability/reactivity of the systems.

The goal of the paper is twofold: (i) to elucidate whether the total energy and the entanglement of the system show up the same kind of chemical phenomena and (ii) to explore the relation quantum entanglement-chemical reactivity. In order to pursue this goal we have studied the water molecule and a simple chemical process, the hydrogenic abstraction reaction. These two chemical systems were chosen because they have few degrees of freedom (namely, they involve molecular systems consisting of only three nuclei) and allow us a transparent illustration of the quantum-entanglement features involved in them. Moreover, being the water a major element of all living things, it is certainly striking that its entanglement-related features properties had been hardly investigated.[43]

The paper is structured as follows. In section 2 the theoretical notions and techniques to compute the entanglement of chemical systems used in this work are described. In section 3, the connection between entanglement and chemical reactivity is explored and discussed for the two systems under consideration. Finally, some conclusions and open problems are given in section 4.

2. QUANTUM ENTANGLEMENT OF CHEMICAL SYSTEMS

It is well-known that the general state for a quantum system, consisting of two distinguishable subsystems (A and B), can be written as a linear superposition of products of their individual states

$$\Psi^{AB} = \sum_{m=1}^{M}\sum_{n=1}^{N} c_{mn}\omega_m(A)\psi_n(B) \tag{1}$$

where $\omega_m(A)$ (M-dimensions) and $\psi_n(B)$ (N-dimensions) are the basis of the subsystems A and B, respectively. In order to assess and reveal the correlations between these two subsystems, it is possible to decompose the quantum state in the Schmidt diagonal form

$$\Psi^{AB} = \sum_{l=1}^{L} \lambda_l \chi_l(A)\phi_l(B) \tag{2}$$

where $L \leq \min(M, N)$ and $\chi_l(A)$ and $\phi_l(B)$ are orthonormal bases for A and B, respectively. Physically, eq 2 points out the quantum correlation between subsystems A and B; i.e., if A is found in a given state $\chi_l(A)$, then B has to be found solely in the $\phi_l(B)$ state. This quantum correlation is called entanglement. Note that if $L = 1$ the subsystems are not entangled, otherwise (i.e., $L > 1$) subsystems A and B are entangled. Also note that each subsystem is in a mixed state, described by the corresponding marginal density matrix, $\rho_{A,B} = \mathrm{Tr}_{B,A}(|\Psi^{AB}\rangle\langle\Psi^{AB}|)$. Hence, the amount of entanglement for a pure state $|\Psi^{AB}\rangle$ is quantified by their degree of mixedness exhibited by the marginal density matrices.

One the most fundamental measure of entanglement for pure states is given by the von Neumann entropy of the marginal density matrices:

$$S(\rho_{A,B}) = -Tr(\rho_{A,B}\ln \rho_{A,B}) \tag{3}$$

A correlation measure is based on the idea that a distance between two different states (a given state and a reference state without the desired property) is able to quantify a property of interest,[44] the entanglement in molecules for this particular case. Therefore, based on the fact that a pure state $|\Psi\rangle$ for a system consisting of N identical Fermions is separable (nonentangled) if it can be represented as a single Slater determinant (Slater rank equal to one), it is feasible to measure the degree of mixedness of a N-Fermionic system by comparing the von Neumann entropy for this particular state (Slater rank equal to one) with another state that cannot be expressed as a single Slater determinant.

To determine the amount of entanglement for a particular state, $|\Psi\rangle$, we obtain the single particle reduced density matrix for a given N-Fermionic system

$$\rho_r = Tr_{2,\ldots,N}(|\Psi\rangle\langle\Psi|) \tag{4}$$

and employ eq 3 in order to calculate the von Neumann entropy of the first-order reduced density matrix

$$S[\rho_r] = -Tr(\rho_r \ln \rho_r) \tag{5}$$

This expression obeys

$$S[\rho_r] \geq \ln N \tag{6}$$

with equality verified if and only if the N-Fermion pure state has Slater rank one. This inequality indicates that correlations, between N-Fermions, that are due solely to the antisymmetric character of the Fermi statistics do not contribute to a quantum entangled state.[45−49] Therefore, the amount of entanglement exhibited by an N-Fermionic state corresponds to the quantum correlations that the state has on top of the minimum ones necessary to satisfy the antisymmetric constraint of the Fermionic wave function:

$$\xi[|\Psi\rangle] = S[\rho_r] - \ln N \tag{7}$$

which defines a quantitative measure of the amount of entanglement exhibited by a pure state $|\Psi\rangle$ of a system of N identical Fermions. This is a non-negative quantity that vanishes if and only if the state $|\Psi\rangle$ is not entangled.

To quantify entanglement in chemical systems, it is desirable to reformulate the expressions above in the context of quantum chemistry. Foremost, recall that the first-order reduced density matrix is usually normalized to the total number of electrons N, its eigenfunctions are called natural spin orbitals,[50−52] and the associated eigenvalues are the natural spin occupation numbers

DOI: 10.1021/acs.jctc.5b00390
J. Chem. Theory Comput. 2015, 11, 5144−5151

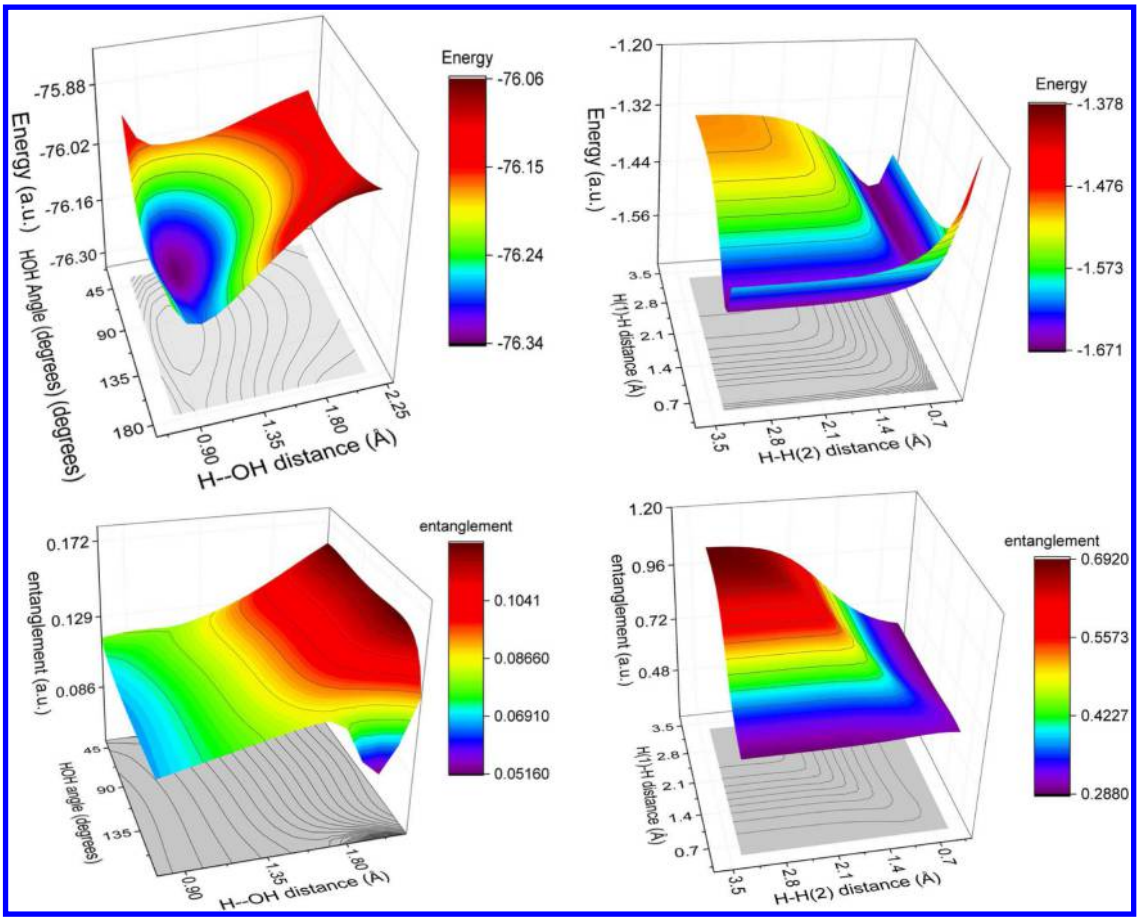

Figure 1. Hypersurfaces and entanglement values for the water molecule (left) and hydrogenic abstraction reaction (right).

n_i^γ (for a closed shell system $i = 1, ..., M$; where M stands for the number of orbitals and γ for the α or β spin channels). Note that the natural spin occupation numbers lies in the range $0 \leq n_i^\gamma \leq 1$ and, as we mentioned before, they are normalized to N; i.e., $\sum_{i,\gamma} n_i^\gamma = N$. From these eigenvalues, it is convenient to (re)normalize the first-order reduced density matrix ρ_r to 1, so that

$$\lambda_i^\gamma = \frac{n_i^\gamma}{N} \tag{8}$$

As a consequence the von Neumann entropy (eq 5), for a closed-shell system, is expressed as

$$S[\rho_r] = -\left(\sum_i^M \frac{n_i^\alpha}{N} \ln \frac{n_i^\alpha}{N} + \frac{n_i^\beta}{N} \ln \frac{n_i^\beta}{N} \right) \tag{9}$$

It is worth noting that a closed-shell molecular (or atomic) system is commonly represented by a double occupied density matrix $\rho_r^{(DO)}$ with eigenvalues $\lambda_i^{(DO)}$ fulfilling the condition $\sum_i \lambda_i^{(DO)} = 1$, and $\lambda_i^{(DO)}/2 = n_i^\alpha/N = n_i^\beta/N$. Therefore, it is more convenient to define eq 9 in terms of a double occupied density matrix

$$S[\rho_r^{DO}] = -\sum_i^M \lambda_i^{(DO)} \ln \lambda_i^{(DO)} \tag{10}$$

From eqs 7 and 10, it is readily seen that

$$\xi[|\Psi\rangle] = S[\rho_r^{(DO)}] - \ln \frac{N}{2} \tag{11}$$

is a suitable measure for quantifying the degree of mixedness of a chemical system.

3. RESULTS AND DISCUSSION

The aim of this work, as already mentioned in section 1, resides in explaining the following entanglement-related chemical features in two simple chemical models: (i) the energetic stability of the water molecule through the hypersurface that arises when geometrical parameters are modified and (ii) the chemical passage from reactants to products in the hydrogenic abstraction reaction. All calculations, that are required to determine the multiconfigurational wave functions necessary to account for the entanglement measures, were carried out at the CISD = full/aug-cc-pvtz level of theory with the Gaussian 09[53] suite of programs.

To provide with a physical explanation of the behavior of the quantum entanglement measure across the hypersurface of the water molecule and the path of the hydrogenic abstraction reaction, we have employed fundamental physical descriptors of the molecular density, the molecular electrostatic potential (MEP) and the atomic electric potentials associated with the basins of the MEP (see below). Both properties are good density descriptors of chemical reactivity, i.e., a higher/lower electric potential (negative) is associated with a lower/higher capacity to gain negative electron charge. Interestingly, bonding situations occur when the difference between the atomic electric potentials of two or more species, either atoms or molecular fragments, become maximum at a specific region of the chemical region of interest.[54]

DOI: 10.1021/acs.jctc.5b00390
J. Chem. Theory Comput. 2015, 11, 5144−5151

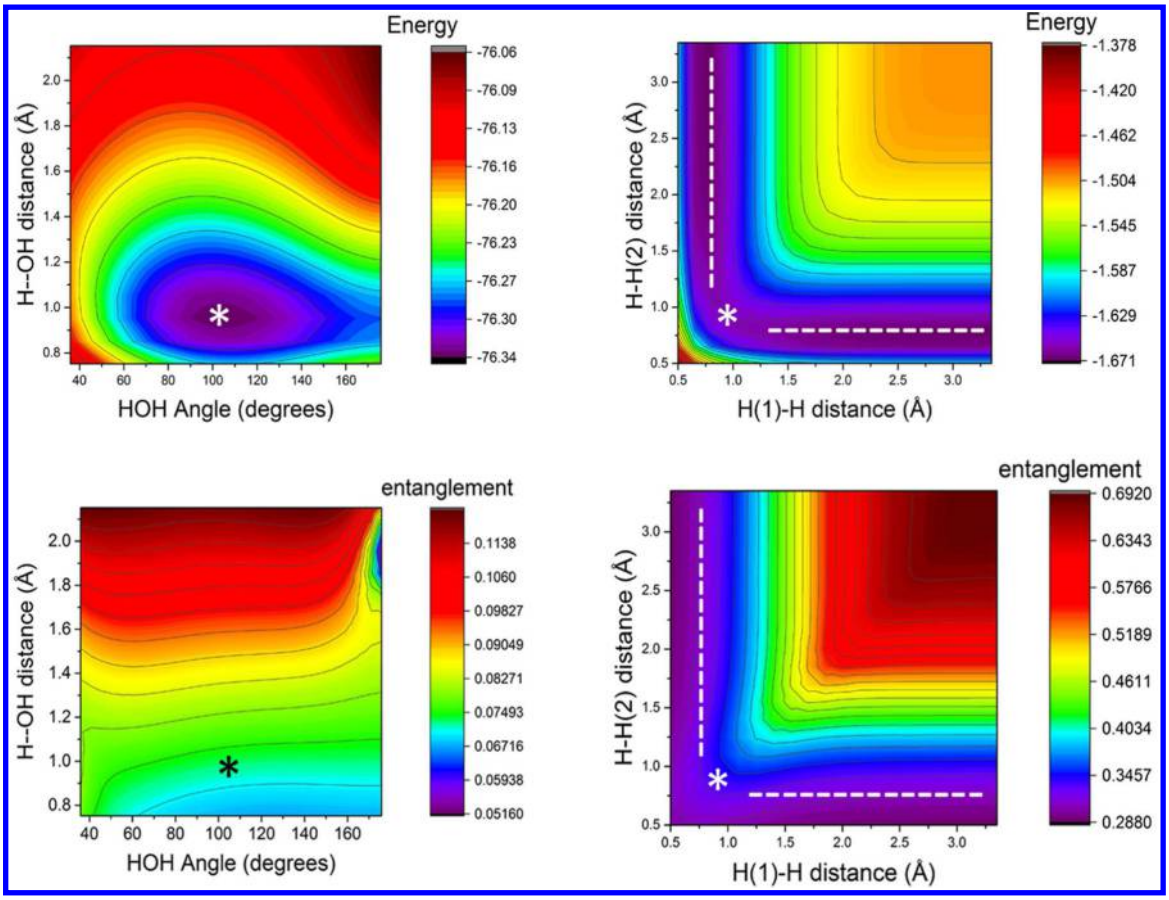

Figure 2. Contour maps for total energy and entanglement of the water molecule (left) and the hydrogenic abstraction reaction (right).

The MEP represents the molecular potential energy of a test charge (proton) at a particular location near a molecule, say at nucleus A. Then, the atomic electrostatic potential, V_A, is defined as

$$V_A = \sum_{B \neq A} \frac{Z_B}{|\mathbf{R}_B - \mathbf{R}_A|} - \int \frac{\rho(\mathbf{r}')\, d\mathbf{r}'}{|\mathbf{r} - \mathbf{r}'|} \tag{12}$$

where $\rho(\mathbf{r})$ is the molecular electron density and Z_A is the nuclear charge on atom A, located at R_A. Hence, a negative electrostatic potential corresponds to the attraction of the proton by the spatial region of electron molecular density that arises from lone pairs, pi-bonds, etc. Positive electrostatic potential corresponds to repulsion of the proton by the atomic nuclei in regions where low electron density exists and the nuclear charge is not completely screened. A charge fitting procedure is employed to extract atomic charges from molecular wave functions the MEP is mapped to the electron density that is obtained by use of ab initio methods. The nonbonded atomic electric potentials (ϵ_i) along with the fitted atomic charges (q_i) will be employed throughout this study according to the CHELPG method.[55] Atomic units are employed throughout.

For the water molecule, the procedure consists on distorting the angle of a water molecule (in steps of 5° from 35.87° to 175.87°) and to elongate the bond distance between one hydrogen and oxygen (in steps of 0.1 Å from 0.75 to 2.15 Å); meanwhile, the bond distance from the remaining hydrogen was partially optimized in order to acquire the most stable molecular structure that preserves the two aforementioned geometrical parameters.

The hydrogen abstraction reaction involves a more intricate process. This chemical reaction $H^{\bullet} + H_2 \rightarrow H_2 + H^{\bullet}$ is the simplest radical abstraction reaction involving a free radical as a reactive intermediate, the atomic hydrogen in this case. The hypersurface for this reaction was obtained by increasing, or decreasing, the bond distance between the entering (leaving) hydrogen with the central hydrogen (the bond distances were modified by steps of 0.15 Å from 0.5 to 3.35 Å). This process was carried out by maintaining a constant value of 180° for the internal angle between the three nuclei. We have chosen to study the hypersurface of this reaction, instead of characterizing intrinsic reaction coordinate path (IRC), in order to gain more knowledge about different chemical processes and their connection with quantum entanglement; i.e., we hope be able to comprehend in which way a chemical process affects the entanglement or, even better, how a chemical process is affected by the entanglement.

Plots in 3D have been generated to represent the energy and the entanglement for both processes under study. Figure 1 represents the energetic behavior of the water molecule (top-left) as compared with the entanglement behavior of the system (bottom-left), as well as the energetic hypersurface of the hydrogen abstraction reaction (top-right) and its entanglement values (bottom-right). We can observe from this figure that both quantities (energy and entanglement) have a completely different behavior, e.g., the energy clearly reveals what is the stable geometry for the water molecule (0.96 Å and 104.5°), while the entanglement distinguishes different regions of the water hypersurface which we will explain below.

DOI: 10.1021/acs.jctc.5b00390
J. Chem. Theory Comput. 2015, 11, 5144−5151

In order to gain insight into the entanglement aspects of the hypersurface of both models, in Figure 2, we have depicted contour maps for the total energy and the entanglement measure following the same order as Figure 1.

For the water molecule (Figure 2, left-top and -bottom), the energetically stable geometry has been signaled with a star symbol. The most relevant aspect is that the entanglement does not reflect the same physical situation of stability in an energetic sense. An analogous situation is observed for the hydrogen abstraction reaction (Figure 2, right-top and -bottom) where the IRC path (dashed line) and the TS (star symbol) are represented. Hence, the physical behavior represented by the entanglement measure corresponds to a different meaning related to the mixedness of the water states.

The energy behavior of the water molecule and the hydrogenic abstraction reaction has been extensively analyzed in the literature, and hence, we will only focus on the entanglement behavior. The general observation for these chemical systems are the following:

(i) For the water molecule (Figure 2 bottom-left), the value of entanglement increases as the H−OH distance is increasing, except for a small region located at large distance and wide angle. Note that the opposite is also observed, i.e., for small H−OH distances the entanglement decreases beyond the region of energetic stability of water, which allows us to conclude that entanglement does not reflect this specific stability. Special attention must be paid to the lowest entanglement region observed at the range of 180° and 1.9 Å. It will be discussed below in connection with Figure 3.

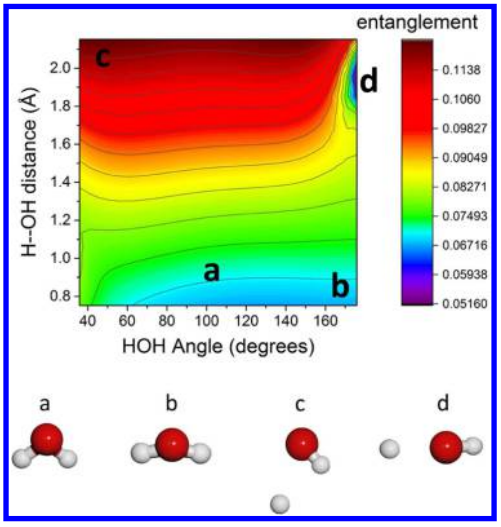

Figure 3. Entanglement hypersurface for the water molecule model.

(ii) For the hydrogenic abstraction reaction we can observe low entanglement region beyond the IRC path toward shorter H−H distances. As it has been observed in a previous study,[40] a METS is observed, corresponding to a maximum mixed state (star symbol). It also must be noted that higher entanglement values are observed outside the IRC path toward larger H−H distances. It is interesting to note that the entanglement reveals multiple reaction paths corresponding to different METS for a given trajectory (at shorter H−H distance).

In Figures 3 and 4 we have depicted the contour map of the entanglement measures for the water molecule and the hydrogenic abstraction reaction, respectively, wherein some representative molecular geometries are shown in order to grasp the electronic response of nuclei rearrangements in terms of entanglement.

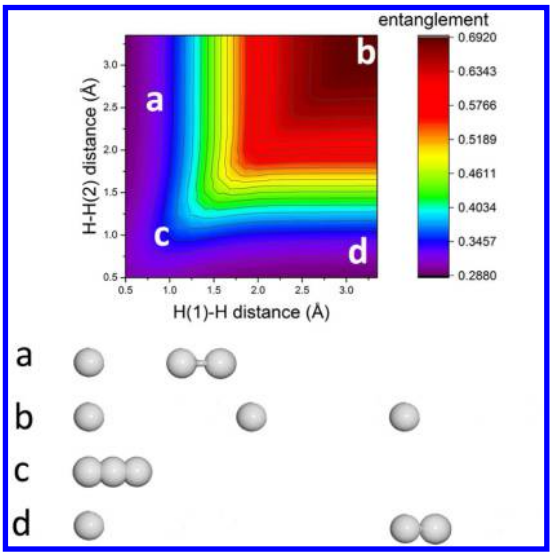

Figure 4. Entanglement hypersurface for the hydrogen abstraction reaction.

It is observed from Figure 3 that the energetically stable molecular geometry does not correspond to a critical point at the entanglement hypersurface (**structure a**). For the case of **structure b** we observe that it holds lower values of entanglement than **structure a**, whereas **structure c** behaves in the opposite way. To obtain both structures, **structure b** and **structure c**, larger values of energy are required corresponding to higher excited states. The lowest value of entanglement corresponds to **structure d**.

Here we would like to emphasize that local minima observed in the hypersurface of entanglement, at a bond distance of 1.8 to 2.0 Å and internuclear angle of 180°, is due to the bond cleavage process. We have verified this by performing a chemical reactivity analysis of the fragments of the molecule (H-leaving, oxygen, OH−, and H_2O) by employing the molecular electrostatic potential (MEP) along with the total dipole moment of the molecule, see Figures 5 and 6 respectively (included in the revised version). According to Figure 5, the water molecule (top-left) shows the nucleophilic character at its energetically stable configuration (in red) and the opposite (electrophilic behavior) at the onset of the bond cleavage region (in blue) witnessing a dramatic chemical change in this region. At the top-right of Figure 5 we depicted the chemical behavior of the OH- fragment, showing a somewhat constant nucleophilic power as the molecule approaches the bond-breaking region. On the other hand, the electric potentials of the leaving hydrogen (Figure 5, bottom-right) and the oxygen atom (Figure 5, bottom-left) show that at the onset of the bond cleavage region (1.6 Å) both atomic species behave in an opposite manner, i.e., whereas the hydrogen holds an electrophilic character (maximum capacity to acquire charge) the oxygen atom possesses a nucleophilic behavior (minimum capacity) and this effect is completely reversed as the dissociation process takes place in such a way

DOI: 10.1021/acs.jctc.5b00390
J. Chem. Theory Comput. 2015, 11, 5144−5151

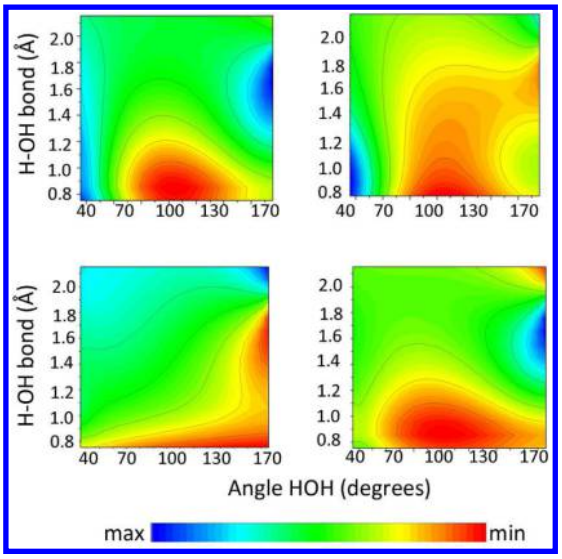

Figure 5. Electric fragment potentials for H_2O (top-left) and OH (top-right) and electric atomic potentials for O (bottom-left) and H-leaving (bottom-right).

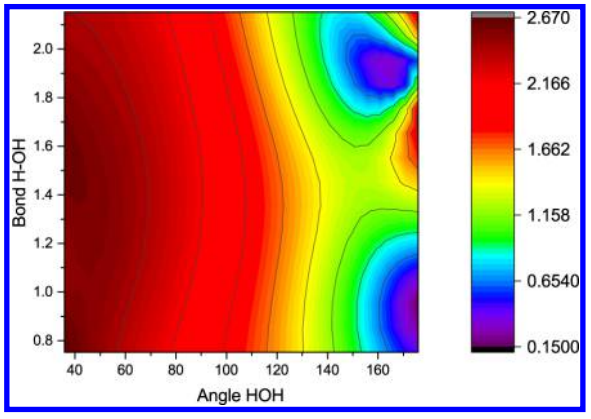

Figure 6. Dipole moment for the water molecule.

that oxygen atom shows its maximum capacity to attract charge whereas the hydrogen atom diminishes this electric capacity beyond 2.0 Å. The above is clearly apparent from the dipole moment (Figure 6) showing a dramatic decrease of its value when the molecule is breaking apart, witnessing the electrostatic balance arising the bond rupture. In spite of the fact that bond-breaking of is also observed at different regions of the hypersurface, for instance at **structure d** in Figure 3, the chemical situation is completely different since at an internuclear angle of 180° the electrostatic effects between both hydrogens cancel out when the oxygen atom eclipse its interaction, provoking the unique entanglement features above observed.

It is physically reasonable to think that immediately afterward the bond cleavage occurs at 1.8 Å a new chemical dissociated species is formed. The associated bond rupture causes an instantaneous effect that provokes the reversing of the electric properties of the chemical species and the short lasting effect of the physically separation of the species and this is exactly where the entanglement region shows a very pronounced minima. In quantum information-theoretical terms, the above instantaneous effect causes the wave function to represent a pure state, the one of the independent species, witnessed by the dropping off the entanglement (local minima at 1.8−2.0 Å). Afterward, both species remain entangled and its wave function represents the mixed state that explains the increasing behavior of the von Neumann measure beyond 2.0 Å. Of course, at some point entanglement should get constant as the separation distance tends to infinity, although this is not shown in the above-mentioned Figures. It is interesting to mention that a similar behavior was observed in diatomic molecules in analyzing its dissociation process to understand the bond cleavage region in terms of quantum entanglement[33]

For the sake of completeness we have found it interesting to plot the correlation energy of the water molecule (Figure 7). We can observe that both quantities behave in a similar manner, except for the minimum entanglement region detected in **structure d**.

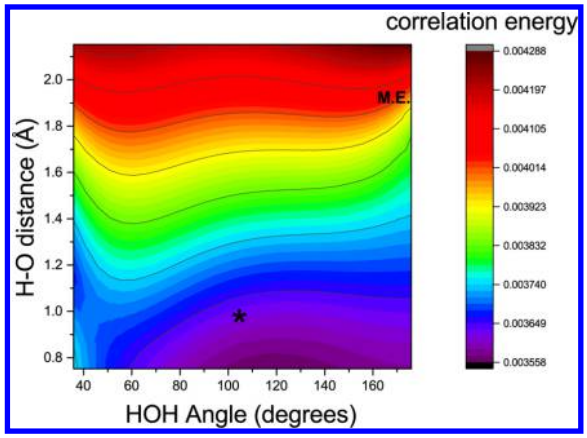

Figure 7. Correlation energy for the water molecule model.

The hypersurface of entanglement for the hydrogen abstraction reaction (Figure 4) reflects that the minimum-energy **structure a** does not hold a critical value for the entanglement. As a matter of fact, the maximally entangled state corresponds to the most-separated molecular-geometry **structure b**, and the less entangled state is related to the particular situation of a long distance interaction between two subsystems associated with **structure d**. Note that entanglement, as a purely quantum effect, does not depend on the interatomic distance beyond the values given by **structure b**, where the entanglement reaches a constant value. Note that **structure c** holds a chemical significance to represent the TS of the reaction (it also corresponds to the maximally entangled state along the IRC path; see the work of Esquivel et al.[40]).

The most relevant observation is that quantum entanglement could be associated with the chemical reactivity of the system, i.e., highly reactive chemical structures have large values of entanglement in the sense that a reactive molecule possesses the capability to convert from one system to other as well to react with different chemical species. From a quantum point of view, these correspond to maximally mixed states. For instance, the TS corresponds to the maximally entangled states along the IRC path (see the work of Esquivel et al.[40]). Besides it has been shown in Figure 4 that there are many other chemical paths with higher maximally entangled transition states (saddle points of nth order) which correspond to chemical reactions of higher excited states, and hence more reactive. On the other hand, lower values of entanglement would be associated with less reactive chemical species. For instance, the reactants and products of the hydrogenic abstraction reactions (see **structure**

DOI: 10.1021/acs.jctc.5b00390
J. Chem. Theory Comput. 2015, 11, 5144−5151

a in Figure 4) and the aqueous chemical species representing the **structure d** in Figure 3.

Finally, it is worth mentioning that in order to reinforce the results of the study to employ quantum entanglement as a chemical witness of reactivity for the molecule of water, we have performed different testing in four different directions: (i) to assess the utility of calculating wave function dependent quantities such as entanglement through the superposition of spin unrestricted rank-one determinants (UHF wave function), (ii) to test the validity of other type of methods (MRCI, CC, QCI) in calculating quantum information measures, (iii) to verify the robustness of our CI-type calculations through a basis-set sensitivity analysis, and (iv) to assess the capability of quantum entanglement in detecting hydrogen-bonding. Summarizing these results we may conclude that (i) spin contamination effect in the UHF method forces the spin-projection of the wave function in such a way that entanglement does not produce any physically meaningful behavior, (ii) by testing other methodologies (CASSCF, CC, and QCISD) we concluded that these produce reasonable representations for the energy profile at the dissociation region (at the H−O−H angle of 180° as the bond increases) and they seem to indicate the existence of the bond-cleavage region although not as clearly depicted as the variational CI methods do, (iii) a sensitivity analysis by using a set of basis sets of increasing quality from CISD/6-31 through CISD/aug-cc-pvtz we observed that CI-type wave functions accurately represent the dissociation region of the energy and the bond cleavage region, and finally (iv) we have also tested the utility of quantum entanglement in detecting hydrogen bonding in a different chemical system (the HF dimer) showing that this interaction is detected through a maximum of the von Neumann entanglement measure. Details of the aforementioned results have been included in the Supporting Information and part of them will be published elsewhere.

4. CONCLUSIONS

Throughout the computation and study of the two selected chemical models (the water molecule and the hydrogenic abstraction reaction), we have gained a deeper understanding about the role played by entanglement on molecular systems and chemical processes. The most important result of our study is that the entanglement phenomenon could be associated with the chemical reactivity of the process.

In summary, we have shown that quantum entanglement fully describes chemical reactivity as we have tested in two different chemical situations:

- Minima of entanglement: As witnessed in the water molecule, once the bond cleavage occurs at 1.8 Å, a new chemical dissociated species is formed. The associated bond rupture causes an instantaneous effect that provokes the reversing of the electric properties of the chemical species and the short lasting effect of the physically separation of the species; this is exactly where the entanglement region shows a very pronounced minima. In quantum information-theoretical terms, the above instantaneous effect causes the wave function apparently to represent a pure state, the one of the independent species, witnessed by the dropping off the entanglement (local minima at 1.8−2.0 Å. Afterward, both species remain entangled and its wave function represents the mixed state that explains the increasing behavior of the von Neumann measure beyond 2.0 Å.
- Maxima of entanglement: Highly reactive chemical structures have large values of entanglement in the sense that a reactive molecule possesses the capability to convert one state of the system into another, as well to react with different chemical species. These correspond to maximally mixed states. For instance, the TS corresponds to the maximally entangled states along the IRC as it is tested in this work with the hydrogenic abstraction reaction. Also, as it was mentioned above, maxima of entanglement might also describe hydrogen-bonding in a different chemical situation of medium to long-range interactions.

■ ASSOCIATED CONTENT

Supporting Information

The Supporting Information is available free of charge on the ACS Publications website at DOI: 10.1021/acs.jctc.5b00390.

Figures A−E (PDF)

■ AUTHOR INFORMATION

Corresponding Authors

*E-mail: gamoles@gmail.com (M.M.-E.).
*E-mail: esquivel@xanum.uam.mx (R.O.E.).
*E-mail: slopezrosa@us.es (S.L.-R.).
*E-mail: dehesa@ugr.es (J.S.D.).

Notes

The authors declare no competing financial interest.

■ ACKNOWLEDGMENTS

R.O.E. thanks J.S.D. and GENIL-SPR at the University of Granada for financial support during the 2014−2015 period. Also, we acknowledge financial support through Mexican grants from CONACyT CB-2009-01/132224, PROMEP-SEP and Spanish grants FIS2011-24540, FIS2014-59311P, FIS2014-54497P, and P11-FQM7276. J.S.D. belongs to the Andalusian research group FQM-0207, R.O.E. to FQM-020, and S.L.-R to FQM-239. Allocation of supercomputing time from Laboratorio de Supercómputo y Visualización at UAM, Sección de Supercomputación at CSIRC Universidad de Granada, and Departamento de Supercómputo at DGSCA-UNAM is gratefully acknowledged.

■ REFERENCES

(1) Tichy, M.; Mintert, F.; Buchleitner, A. *J. Phys. B: At., Mol. Opt. Phys.* **2011**, *44*, 192001.
(2) Nielsen, M. A.; Knill, E.; Laflamme, R. *Nature* **1998**, *396*, 52.
(3) Al-Khalili, J.; McFadden, J. *Life on the Edge: The Coming of Age of Quantum Biology*; Bantam Press: New York, 2014.
(4) Ball, P. *Nature* **2011**, *474*, 272.
(5) Pauls, J. A.; Zhang, Y.; Berman, G. P. *Phys. Rev. E* **2013**, *87*, 062704.
(6) Zhu, J.; Kais, S.; Aspuru-Guzik, A.; et al. *J. Chem. Phys.* **2012**, *137*, 074112.
(7) Legeza, O.; Solyom, J. *Phys. Rev. B: Condens. Matter Mater. Phys.* **2003**, *68*, 195116.
(8) Legeza, O.; Solyom, J. *Phys. Rev. B: Condens. Matter Mater. Phys.* **2004**, *70*, 205118.
(9) Rissler, J.; Noack, R. M.; White, S. R. *Chem. Phys.* **2006**, *323*, 519.
(10) Wei, Q.; Kais, S.; Friedrich, B. *J. Chem. Phys.* **2011**, *135*, 154102.
(11) Wang, H. F.; Kais, S. *Chem. Phys. Lett.* **2006**, *421*, 338.
(12) Kais, S. *Adv. Chem. Phys.* **2007**, *134*, 493.

DOI: 10.1021/acs.jctc.5b00390
J. Chem. Theory Comput. 2015, 11, 5144−5151

(13) Dehesa, J. S.; Koga, T.; Yañez, R. J.; Plastino, A. R.; Esquivel, R. O. *J. Phys. B: At., Mol. Opt. Phys.* **2012**, *45*, 015504.
(14) Dehesa, J. S.; Koga, T.; Yañez, R. J.; Plastino, A. R.; Esquivel, R. O. *J. Phys. B: At., Mol. Opt. Phys.* **2012**, *45*, 239501.
(15) Lin, Y. C.; Lin, C. Y.; Ho, Y. K. *Phys. Rev. A: At., Mol., Opt. Phys.* **2013**, *87*, 022316.
(16) Pipek, J.; Nagy, I. *Phys. Rev. A: At., Mol., Opt. Phys.* **2009**, *79*, 052501.
(17) Harshman, N. L.; Flynn, W. F. *Quant. Inf. Comp.* **2011**, *11*, 278.
(18) Kościk, P.; Okopińska, A. *Phys. Lett. A* **2010**, *374*, 3841.
(19) Lin, Y. C.; Ho, Y. K. *Can. J. Phys.* **2015**, *93*, 646 (and references therein).
(20) Kościk, P.; Okopińska, A. *Few-Body Syst.* **2014**, *55*, 1151 (and references therein).
(21) Wang, H.; Kais, S. *Isr. J. Chem.* **2007**, *47*, 59.
(22) Nazmitdinov, R. G.; Simonovic, N. S.; Plastino, A. R.; Chizhov, A. V. *J. Phys. B: At., Mol. Opt. Phys.* **2012**, *45*, 205503.
(23) Majtey, A. P.; Plastino, A. R.; Dehesa, J. S. *J. Phys. A: Math. Theor.* **2012**, *45*, 115309.
(24) Sadhukhan, P.; Bhattacharjee, S. M. *J. Phys. A: Math. Theor.* **2012**, *45*, 425302.
(25) Schröter, S.; Friedrich, H.; Madronero, J. *Phys. Rev. A: At., Mol., Opt. Phys.* **2013**, *87*, 042507.
(26) Carlier, F.; Mandilara, A.; Sarfati, A. *J. Phys. B: At., Mol. Opt. Phys.* **2007**, *40*, S199.
(27) Osenda, O.; Serra, P. *Phys. Rev. A: At., Mol., Opt. Phys.* **2007**, *75*, 042331.
(28) Osenda, O.; Serra, P. *J. Phys. B: At., Mol. Opt. Phys.* **2008**, *41*, 065502.
(29) Coe, J. P.; Sudbery, A.; D'Amico, I. *Phys. Rev. B: Condens. Matter Mater. Phys.* **2008**, *77*, 205122.
(30) Gavrilik, A. M.; Mishchenko, Y. A. *J. Phys. A: Math. Theor.* **2013**, *46*, 145301.
(31) Benavides-Riveros, C. L.; Gracia-Bondía, J. M.; Springborg, M. *Phys. Rev. A: At., Mol., Opt. Phys.* **2013**, *88*, 022508.
(32) Benavides-Riveros, C. L.; Gracia-Bondía, J. M.; Várilly, J. C. *Phys. Rev. A: At., Mol., Opt. Phys.* **2012**, *86*, 022525.
(33) Esquivel, R. O.; Flores-Gallegos, N.; Molina-Espíritu, M.; Plastino, A. R.; Dehesa, J. S.; Angulo, J. C.; Antolín, J. *J. Phys. B: At., Mol. Opt. Phys.* **2011**, *44*, 175101.
(34) Mottet, M.; Tecmer, P.; Boguslawski, K.; Legeza, O.; Reiher, M. *Phys. Chem. Chem. Phys.* **2014**, *16*, 8872.
(35) Boguslawski, K.; Tecmer, P.; Barcza, G.; Legeza, O.; Reiher, M. *J. Chem. Theory Comput.* **2013**, *9*, 2959.
(36) Legeza, O.; Solyom, J. *Phys. Rev. Lett.* **2006**, *96*, 116401.
(37) Murg, V.; Verstraete, F.; Schneider, R.; Nagy, P. R.; Legeza, O. *J. Chem. Theory Comput.* **2015**, *11*, 1027.
(38) Fertitta, E.; Paulus, B.; Barcza, G.; Legeza, O. *Phys. Rev. B: Condens. Matter Mater. Phys.* **2014**, *90*, 245129.
(39) Esquivel, R. O.; Angulo, J. C.; Dehesa, J. S.; Antolín, J.; López-Rosa, S.; Flores-Gallegos, N.; Molina-Espíritu, M.; Iuga, C. *Recent Advances Toward the Nascent Science of Quantum Information Chemistry in Information Theory: New Research*; Deloumeaux, P., Gorzalka, J. D., Eds.; Nova Science Publishers, Inc., 2012; Chapter 8 pp 297−334.
(40) Esquivel, R. O.; Molina-Espíritu, M.; Plastino, A. R.; Dehesa, J. S. *Int. J. Quantum Chem.* **2015**, *115*, 1417.
(41) Kotz, J. C.; Treichel, P. M.; Townsend, J. R. *Chemistry and Chemical Reactivity*; Thomson Brooks/Cole, 2012.
(42) Esquivel, R. O.; Angulo, J. C.; Antolín, J.; Dehesa, J. S.; López-Rosa, S.; Flores-Gallegos, N. *Phys. Chem. Chem. Phys.* **2010**, *12*, 7108.
(43) Pang, X. F. *WATER. Molecular Structure and Properties*; World Scientific: New York, 2014.
(44) Modi, K.; Paterek, T.; Son, W.; Vedral, V.; Williamson, M. *Phys. Rev. Lett.* **2010**, *104*, 080501.
(45) Ghirardi, G.; Marinatto, L. *Phys. Rev. A: At., Mol., Opt. Phys.* **2004**, *70*, 012109.
(46) Ghirardi, G.; Marinatto, L.; Weber, T. *J. Stat. Phys.* **2002**, *108*, 49.
(47) Naudts, J.; Verhulst, T. *Phys. Rev. A: At., Mol., Opt. Phys.* **2007**, *75*, 062104.
(48) Oliveira, V. C. G.; Santos, H. A. B.; Torres, L. A. M.; Souza, A. M. C. *Int. J. Quantum Inf.* **2008**, *6*, 379.
(49) Plastino, A. R.; Manzano, D.; Dehesa, J. S. *EPL (Europhysics Letters)* **2009**, *86*, 20005.
(50) Lowdin, P. O. *Phys. Rev.* **1955**, *97*, 1474.
(51) Lowdin, P. O.; Shull, H. *Phys. Rev.* **1956**, *101*, 1730.
(52) Lowdin, P. O. *Adv. Quantum Chem.* **1970**, *5*, 185.
(53) Frisch, M. J.; Trucks, G. W.; Schlegel, H. B.; Scuseria, G. E.; Robb, M. A.; Cheeseman, J. R.; Scalmani, G.; Barone, V.; Mennucci, B.; Petersson, G. A.; Nakatsuji, H.; Caricato, M.; Li, X.; Hratchian, H. P.; Izmaylov, A. F.; Bloino, J.; Zheng, G.; Sonnenberg, J. L.; Hada, M.; Ehara, M.; Toyota, K.; Fukuda, R.; Hasegawa, J.; Ishida, M.; Nakajima, T.; Honda, Y.; Kitao, O.; Nakai, H.; Vreven, T.; Montgomery, J. A., Jr.; Peralta, J. E.; Ogliaro, F.; Bearpark, M.; Heyd, J. J.; Brothers, E.; Kudin, K. N.; Staroverov, V. N.; Kobayashi, R.; Normand, J.; Raghavachari, K.; Rendell, A.; Burant, J. C.; Iyengar, S. S.; Tomasi, J.; Cossi, M.; Rega, N.; Millam, J. M.; Klene, M.; Knox, J. E.; Cross, J. B.; Bakken, V.; Adamo, C.; Jaramillo, J.; Gomperts, R.; Stratmann, R. E.; Yazyev, O.; Austin, A. J.; Cammi, R.; Pomelli, C.; Ochterski, J. W.; Martin, R. L.; Morokuma, K.; Zakrzewski, V. G.; Voth, G. A.; Salvador, P.; Dannenberg, J. J.; Dapprich, S.; Daniels, A. D.; Farkas, Ö; Foresman, J. B.; Ortiz, J. V.; Cioslowski, J.; Fox, D. J. *Gaussian 09*, Revision D.01; Gaussian, Inc.: Wallingford CT, 2009.
(54) Esquivel, R. O.; Molina-Espíritu, M.; Dehesa, J. S.; Angulo, J. C.; Antolín, J. *Int. J. Quantum Chem.* **2012**, *112*, 3578−3586.
(55) Breneman, M.; Wiberg, K. B. *J. Comput. Chem.* **1990**, *11*, 361.

DOI: 10.1021/acs.jctc.5b00390
J. Chem. Theory Comput. 2015, 11, 5144−5151